Population Modeling of Filgrastim PK-PD in Healthy Adults Following Intravenous and Subcutaneous Administrations

Wojciech Krzyzanski, PhD, Pawel Wiczling, PhD, Phil Lowe, PhD, Etienne Pigeolet, PhD, Martin Fink, PhD, Alexander Berghout, MD, and Sigrid Balser, PhD

Filgrastim is a recombinant human granulocyte colony stimulating factor (G-CSF) that stimulates production of neutrophils. The objective of this analysis was to develop a pharmacokinetic (PK) and pharmacodynamic (PD) model to account for an increase in G-CSF clearance on multiple dosing because of an increase of the G-CSF receptor-mediated endocytosis. Data from 4 randomized studies involving healthy volunteers were used for analysis. Subjects received filgrastim (Neupogen) via subcutaneous (SC) and intravenous (IV) routes. Filgrastim was administered SC daily for 1 week at 2.5, 5, and 10 μg/kg doses and as single IV infusions (5 μg/kg over 0.5 hours) and SC (1 μg/kg) doses. PK data comprised serum concentration-time measurements and the blood absolute neutrophil count (ANC) was used for PD evaluations. Population nonlinear mixed-effect modeling was done using NONMEM VI (Version 6.1.0, Icon Development Solutions, Ellicott City, Maryland). The model depicted the decaying trend in C_{max} values with repeated doses and an increase in ANC_{max} values consistently with an increase in the G-CSF receptor pool. Simulated time courses of the total clearance exhibited an increasing pattern. The increase in filgrastim clearance on multiple dosing was attributed to the increased neutrophil count in the bone marrow and blood paralleled by an increase in the total G-CSF receptor density.

Keywords: *Granulocyte-colony stimulating factor; neutrophils; granulopoiesis; target-mediated drug disposition; mechanistic models*

Journal of Clinical Pharmacology, 2010;50:101S-112S

Filgrastim is a recombinant methionyl form of human granulocyte-colony stimulating factor (r-metHuG-CSF) derived from *Escherichia coli*. It consists of 175 amino acids and has a molecular weight of 18 800 daltons. The biological activity of filgrastim is identical to the endogenous G-CSF, which controls neutrophil production within the bone marrow by stimulating activation, proliferation, differentiation, and survival of myeloid progenitor cells.[1] The G-CSF mediates its biological actions by binding to a specific cell-surface receptor (G-CSFR). The G-CSFR is present on cells of the neutrophilic granulocyte lineage from the myeloblasts to the mature neutrophils. Binding of the G-CSF to its receptor activates a number of cytoplasmic tyrosine kinases that initiate a cascade of downstream signaling events.[2] The G-CSF-G-CSFR complex is internalized to the endosomal compartments, and either recycled or degraded.[3] It is believed that only a minority of G-CSFRs need to be occupied to elicit maximal biological response.

Neutrophil production in a normal adult human takes place in the bone marrow by a process termed granulopoiesis. It is a continuous process of differentiation, divided in a series of steps based on a morphological appearance of cells. Granulocytic progenitors originated from bone marrow pluripotent stem cells differentiate into the precursor cells myeloblasts, promyelocytes, and myelocytes. These cells are capable of division and constitute the mitotic compartment with the transit time equal to 143 hours.[4] The more mature forms of neutrophil series (in order of age: metamyelocytes, band and polymorphonuclear neutrophils) are incapable of cell division and constitute

From Department of Pharmaceutical Sciences, State University of New York at Buffalo, Buffalo, New York (Dr Krzyzanski); the Department of Biopharmaceutics and Pharmacodynamics, Medical University of Gdansk, Poland (Dr Wiczling); Novartis Pharma AG, Modeling and Simulation, Basel, Switzerland (Dr Lowe, Dr Pigeolet, Dr Fink); and Sandoz Biopharmaceutical Development, Holzkirchen, Germany (Dr Berghout, Dr Balser). Submitted for publication April 14, 2010; revised version accepted May 27, 2010. Address for correspondence: Wojciech Krzyzanski, University at Buffalo, 565B Hochstetter Hall, Buffalo, NY 19426; wk@buffalo.edu.
DOI:10.1177/0091270010376966

the maturing compartment with the transit time equal to 166 hours.[4] From the maturation compartment, cells migrate to the blood. In the blood, cells are distributed approximately equally between circulating (49%) and marginal pools (51%).[5] Cells in the marginal pool move through the vessel wall to enter the tissues (diapedesing). The average neutrophil circulates approximately 10 hours in the blood before diapedesing to the tissues.[6] Once neutrophils leave the blood, they do not return in significant numbers.[4]

The primary effects of G-CSF on normal hematopoietic cells are limited to cells of the neutrophil lineage. G-CSF supports the survival and stimulates the proliferation of neutrophil progenitors and promotes their differentiation into mature neutrophils.[7,8] Additionally, G-CSF causes premature release of neutrophils from the bone marrow as well as enhancement of mature cell function. The mobilizing effect of G-CSF extends on other hematopietic cells in the bone marrow including stem cells.[9] G-CSF also promotes margination of neutrophils.[1] Filgrastim is an agent used therapeutically for treatments of neutropenia associated with chemotherapy, conditions of severe chronic neutropenia, and for the mobilization of hematopoietic stem cells and progenitors for transplantation.[10]

The pharmacokinetics of the G-CSF has been reported to be nonlinear.[11,12] The receptor-mediated binding of the G-CSF followed by internalization and degradation was shown to be an important mode of drug clearance.[13,14] Glomerular filtration and subsequent renal metabolism is a major elimination pathway for G-CSF besides receptor-mediated elimination.[15] The nonlinearity in the G-CSF clearance was modeled by means of the Michaelis-Menten elimination that was independent of the number of neutrophils.[12] In recent models, the receptor-mediated clearance of G-CSF has been accounted for by setting the V_{max} term in the Michaels-Menten equation to be proportional to the circulating neutrophils.[16] Our group has applied the target-mediated drug disposition (TMDD) concept to develop a PK model for G-CSF administered in healthy volunteers.[17] The TMDD has been introduced to account for clearance of drugs that are majorly eliminated by binding to their receptors followed by degradation.[18,19] TMDD PK models were successfully applied to describe nonlinear disposition of monoclonal antibodies[20] and cytokines,[21] including hematopoietic factors such as erythropoietin[22] and thrombopoietin.[23]

Mathematical models for granulopoiesis with G-CSF as a major regulatory factor have been developed to account for dominant mechanisms controlling neutrophil turnover as well as G-CSF pharmacokinetics.[15,24,25] Despite the mathematical complexity, these models would be difficult to apply to analysis of typical clinical data consisting of G-CSF plasma concentrations and absolute neutrophil counts (ANC) without encountering parameter identifiability issues. More parsimonious pharmacodynamic models have been proposed where the ANC data were modeled by a basic indirect response model.[12] Subsequent models included transit compartments accounting for all stages of neutrophil development spanning from metamyelocytes up to circulating neutrophils and implementing all major modes of G-CSF actions on neutrophil progenitor cells.[16]

Our primary objective was to expand our previously developed TMDD pharmacokinetic model for filgrastim administration in healthy volunteers onto a PK-PD model describing also the ANC data.[17] The data included in our analysis comprised both single and multiple IV and SC injections. We observed that the time dependent G-CSF clearance significantly increased following multiple drug administrations. This phenomenon was reported previously[26] and it was attributed to an increase in the G-CSFR pool size because of an increase of cell number in bone marrow precursor and blood neutrophil compartments. Our secondary objective was to include this mechanism in the PK-PD model. We adopted the published models of the neutrophil dynamics and combined them with our TMDD PK model so that the receptor mediated clearance depended on the total neutrophil count. This constitutes a significant improvement of the description of mechanisms of filgrastim clearance provided by existing models. Furthermore, we used computer simulations to explore the impact of neutrophil dynamics on the G-CSF clearance, as well as the time course of the G-CSFR pool.

METHODS

Clinical Study Design

Data from 4 randomized studies involving healthy male (n = 37) and female (n = 30) volunteers were used for analysis. A summary of clinical studies of filgrastim is shown in Table I. Subjects received filgrastim (Neupogen) via SC and IV routes. Filgrastim was administered as repeated SC daily administration for 1 week of 2.5, 5, and 10 μg/kg doses and as single IV infusions (5 μg/kg over 0.5 hours) and SC (1 μg/kg) doses. The samples were analyzed for serum G-CSF using an ELISA assay. The serum G-CSF concentrations below LQ = 0.04 ng/ml were set to the half of LQ (0.02 ng/mL). Only a part of the pretreatment observations were below LQ levels. Serum concentration-time

Table I Summary of Clinical Studies of Filgrastim

Study	Route	N	Doses, µg/kg	Dosing Times, Day of Study
101	SC	16	10	0, 1, 2, 3, 4, 5, 6
102	IV	12	5	0
103	SC	27	2.5 (n = 14) 5 (n = 13)	0, 1, 2, 3, 4, 5, 6
105	SC	12	1	0

SC, subcutaneous; IV, intravenous.

Table II Descriptive Statistics of Patients Enrolled in Clinical Studies of Filgrastim

Name	Descriptive Statistic
Gender	Male, n = 37 Female, n = 30
Race	White, n = 67
Height, m	175.7 (158-205)
Weight, kg	75.4 (56.6-111.8)
Age, y	36.7 (22-53)

records were evaluated from rich sampling profiles consisting of the total of 1778 points. For hematology evaluation, whole blood samples were analyzed. The ANC was calculated as the product of the percentage of neutrophils and the total white blood cell count. Pharmacodynamic data (ANC) were comprised of 1661 points. The descriptive statistics of subjects enrolled in our analysis are presented in Table II.

PK-PD Fixed Effects Model

The schematic representation of the proposed PK-PD model is shown in Figure 1. The free G-CSF concentration C in the serum was assumed to be in an instantaneous equilibrium with the bone marrow and to bind to G-CSF receptors R present on blood and bone marrow neutrophils at a second order rate constant k_{on}, to form drug receptor complex RC. The G-CSF can also be directly eliminated by a glomerular filtration and subsequent renal metabolism represented by a first order elimination rate k_{el}. The endogenous G-CSF was assumed to be continuously produced at a zero-order rate constant k_{GCSF}. The drug receptor complex RC can dissociate at a rate k_{off} or be internalized at a rate k_{int}. The internalized G-CSF receptor complex was assumed to be further degraded in the endosomes and not to recycle as a free receptor and a drug molecule. Because

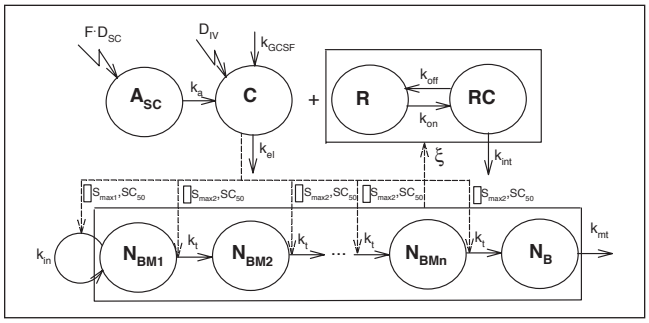

Figure 1. Schematic diagram of the PK-PD model. The model operation and parameters are explained in the Methods section. The open boxes represent stimulatory effects of filgrastim described by the Hill functions, Equation 10. The upper box containing R and RC stands for the total receptor concentration R_{tot}. The lower box containing all neutrophil compartments in the bone marrow and blood represents the total neutrophil count in these tissues $N_{BM} + N_B$. The total neutrophil count controls R_{tot} (broken arrow) according to Equation 6.

the identification of the binding parameters in the presence of the PD data was difficult, the TMDD model of G-CSF disposition was further reduced to a rapid binding form[27] where the free drug and receptor concentrations are replaced by total concentrations because of the quasi-equilibrium assumption:

$$\frac{C \cdot R}{RC} = \frac{k_{off}}{k_{on}} = K_D \qquad (1)$$

The differential equation describing the total G-CSF concentration $C_{tot} = C + RC$ was:

$$\frac{dC_{tot}}{dt} = Input + k_{GCSF} - k_{el} \cdot C - k_{int} \cdot RC \qquad (2)$$

where input accounted for both IV and SC administration of filgrastim as follows:

$$Input = \begin{cases} Dose / V_D / t_{inf}, & \text{for } t \le t_{inf};\ IV \\ 0, & \text{for } t > t_{inf};\ IV \\ k_a \cdot F \cdot Dose / V_D \cdot e^{-k_a \cdot t}, & SC \end{cases} \qquad (3)$$

and k_a denotes the first-order absorption rate constant, F is the bioavailability, and V_D is the volume of distribution. The filgrastim serum concentration was calculated as[27]:

$$C = 0.5 \cdot ((C_{tot} - R_{tot} - K_D) + \sqrt{(C_{tot} - R_{tot} - K_D)^2 + 4 \cdot K_D \cdot C_{tot}}) \qquad (4)$$

and the bound G-CSF complex as[27]:

$$RC = \frac{R_{tot} \cdot C}{K_D + C} \quad (5)$$

where $R_{tot} = R + RC$ is the total concentration of G-CSFR. A key assumption for the structure of the PK-PD model was the relationship between R_{tot} and the neutrophil count. Because G-CSFR is expressed on both bone marrow precursors N_{BM} and circulating neutrophils N_B we assumed that:

$$R_{tot} = \xi \cdot (N_{BM} + N_B) \quad (6)$$

where ξ is a proportionality constant. The neutrophil dynamics was described according to a previously introduced model[16] with a modification of the production rate k_{in}. Instead of a zero-order rate constant, k_{in} was assumed to be a first-order as suggested by models of chemotherapy-induced myelosuppression.[28] The development of neutrophil precursor cells in the bone marrow was described by a sequence of n = 9 transit compartments with a transit rate constant k_t. The model of neurophils in blood comprised of 1 pool with a first-order elimination rate constant k_{mt}. An attempt was made to include additional processes such as mobilization of neutrophil precursors from the bone marrow to the blood, and marginalization of the circulating neutrophils represented by a marginal pool. However, none of these mechanisms were identified with an acceptable precision and were not included in the final model. The PD model equations were as follows:

$$\frac{dN_{BM1}}{dt} = k_{in} \cdot H_1 \cdot N_{BM1} - k_t \cdot H_2 \cdot N_{BM1} \quad (7)$$

$$\frac{dN_{BMi}}{dt} = k_t \cdot H_2 \cdot N_{BMi-1} - k_t \cdot H_2 \cdot N_{BMi},\ i = 2,\ldots,n. \quad (8)$$

$$\frac{dN_B}{dt} = k_t \cdot H_2 \cdot N_{BMn} - k_{mt} \cdot N_B \quad (9)$$

where H_1 and H_2 denote the stimulatory Hill functions

$$H_1 = 1 + \frac{S_{max1} \cdot C}{SC_{50} + C} \text{ and } H_2 = 1 + \frac{S_{max2} \cdot C}{SC_{50} + C} \quad (10)$$

For parsimony reasons, the same potency parameter, SC_{50} (drug serum concentration eliciting 50% of the maximum effect), was used for the G-CSF effect on cell proliferation (k_{in}) and cell maturation (k_t). The total neutrophil count in the bone marrow can be expressed as:

$$N_{BM} = N_{BM1} + \ldots + N_{BMn} \quad (11)$$

The system was assumed to be at a steady-state prior to the administration of the drug. The baseline equations derived from Equations 2, 7, 8, and 9 are as follows:

$$k_{GCSF} = k_{el} \cdot C_0 + k_{int} \cdot RC_0 \quad (12)$$

$$k_{in} = \frac{k_t \cdot H_{20}}{H_{10}} \quad (13)$$

$$N_{BM10} = \ldots = N_{BMn0} \quad (14)$$

$$N_{BMn0} = \frac{k_{mt} \cdot N_{B0}}{k_t \cdot H_{20}} \quad (15)$$

$$RC_0 = \frac{R_{tot0} \cdot C_0}{K_D + C_0} \quad (16)$$

$$H_{10} = 1 + \frac{S_{max1} \cdot C_0}{SC_{50} + C_0} \text{ and } H_{20} = 1 + \frac{S_{max2} \cdot C_0}{SC_{50} + C_0} \quad (17)$$

where C_0 was a baseline serum G-CSF concentration, and $N_{BM10}, \ldots, N_{BMn0}$ are the baseline values for neutrophil precursor compartments in the bone marrow. The baseline total receptor concentration R_{tot0} was calculated as:

$$R_{tot0} = \xi \cdot (N_{BM10} + \ldots + N_{BMn0} + N_{B0}) \quad (18)$$

The baseline values of C_0 and N_{B0} were used in the model as parameters to be estimated. The initial conditions for differential Equations 2, 7, 8, and 9 were set to the following:

$$C_{tot}(0) = C_0 + RC_0,\ N_B(0) = N_{B0},\ \text{and } N_{BMi}(0) = N_{BMn0},\ i = 1,\ldots,n. \quad (19)$$

The estimated fixed effect parameters were F, k_a, k_{el}, V_D, K_D, k_{int}, ξ, k_{mt}, k_t, N_{B0}, SC_{50}, S_{max1}, and S_{max2}.

Population PK-PD Modeling

Population nonlinear mixed-effect modeling was done using NONMEM (Version 6.1.0, Icon Development Solutions, Ellicott City, Maryland) and the Intel Fortran Compiler 9.0. NONMEM runs were executed using Wings for NONMEM (WFN611; http://wfn.sourceforge.net/index.html). The first-order conditional estimation (FOCE) method with interaction was used. The observed concentrations of filgrastim and blood neutrophil counts were defined by the following equations:

$$C_{obs} = C \cdot (1 + \varepsilon_{propC}) + \varepsilon_{addC} \quad (20)$$

$$N_{Bobs} = N_B \cdot (1 + \varepsilon_{propNB}) + \varepsilon_{addNB} \quad (21)$$

where C and N_B were described by Equations 4 and 9 of the basic structural population model, and ε_{prop} and ε_{add} represented the proportional and additive residual random errors. It was assumed that all ε are normally distributed around a mean of 0, with variances denoted by σ^2_{prop} and σ^2_{add}. Interindividual variability (IIV) for the PK-PD parameters was modeled using the following exponential variability model:

$$P = \theta_P \exp(\eta_P) \quad (22)$$

where P is a PK-PD parameter, θ_P is the typical value of this parameter in the population, and η_P is a random effect of that parameter with mean 0 and variance ω_P^2. The IIV was estimated for k_{el}, V_D, k_a, ξ, SC_{50}, S_{max1}, and N_{B0}. The baseline G-CSF concentrations C_0 were fixed at individual pretreatment values. The other parameters were estimated without intersubject variability to reduce the number of parameters in the model.

Goodness-of-fit was evaluated by visual inspection of diagnostic scatter plots, including observed and predicted values versus time, and observed versus population and individual predicted values. The visual predictive performance of the final model was performed by simulating 200 subjects using model parameter estimates. The simulations were done using NONMEM and were presented as 5th, 50th (median), and 95th percentiles along with experimental data.

Simulations

The typical values of PK-PD parameters were used for all simulations. The baseline G-CSF serum concentration was set to the mean baseline of the data C_0 = 0.0246 ng/mL. The simulations included time profiles for R, RC, R_{tot}, C_{tot}, CL_{tot} for dosing regimens 2.5, 5, and 10 µg/kg SC q.d. for 7 days. The total clearance was calculated according to the following equation accounting for linear and receptor mediated elimination[17]:

$$CL_{tot} = k_{el} \cdot V_D + \frac{k_{int} \cdot R_{tot} \cdot V_D}{K_D + C}. \quad (23)$$

A conversion factor of 53.2 pM/ng/mL, calculated based on the filgrastim molecular weight 18.8 kD, was used to express R, RC, R_{tot}, C_{tot} in molar concentration units.

RESULTS

The visual predictive checks of G-CSF concentrations and ANC responses are shown for all dosing schemes in Figures 2 and 3. These plots show that the final PK-PD model described the measured PK-PD data reasonably well. Decreasing concentration peaks and troughs following multiple doses were adequately captured by the PK model. The major misfits of filgrastim concentrations were present for the terminal phases of the multiple dose data. The diagnostic plots in Figure 4 also demonstrate this shortcoming. The ANC data exhibited increases in peak and trough values following multiple dosing. Although the model overall captured the trend in the PD data, the peaks for 1 and 2.5 µg/kg SC data were under-predicted and for 10 µg/kg data were over-predicted. There are 2 mechanisms responsible for an increase in ANC because of exposure to G-CSF: stimulation of the proliferation rate k_{in} and acceleration of the maturation rate k_t. Both are modeled using the Hill function, Equation 10. Although physiologically different, they share the same parameter SC_{50} because of identifiability issues. This was sufficient to describe the individual PD data as shown in the diagnostic plots in Figure 4, but was not enough to eliminate systematic misfits of the ANC peaks.

The parameter estimates obtained by the simultaneous fitting of the PK-PD data are listed in Table III. The typical value of filgrastim absorption rate k_a is 0.602 h^{-1}, and the bioavailability F for the SC administration equals 0.602. The volume of distribution V_D equals 2.42 L. The linear clearance is small with the elimination rate constant k_{el} = 0.152 h^{-1}. Relative standard errors of these estimates do not exceed 17%.

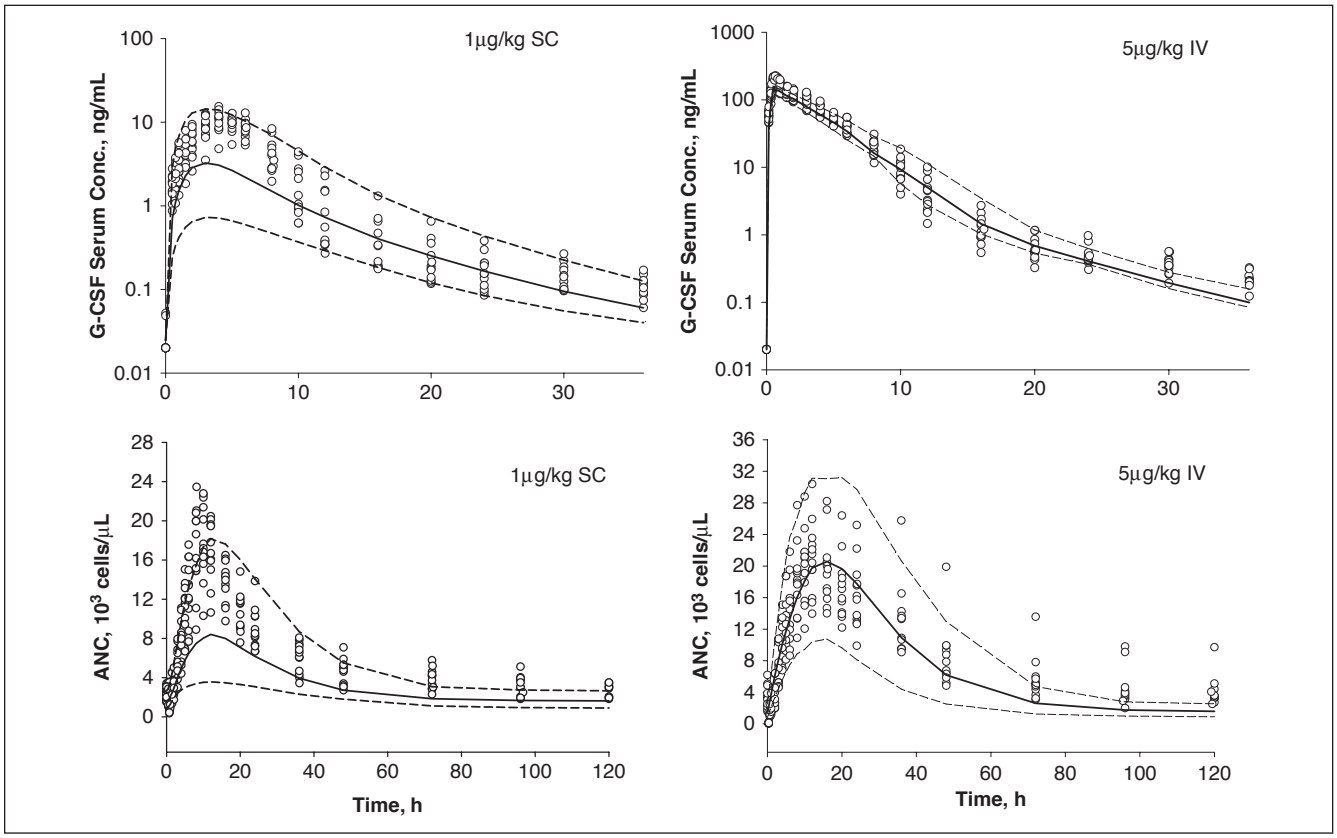

Figure 2. Time courses of filgrastim serum concentrations and ANCs (symbols) following a single administration of 1 µg/kg SC (left) and 5 µg/kg IV (right). The lines represent the 5th, 50th, and 95th percentiles of model-predicted values based on parameter estimates shown in Table III.

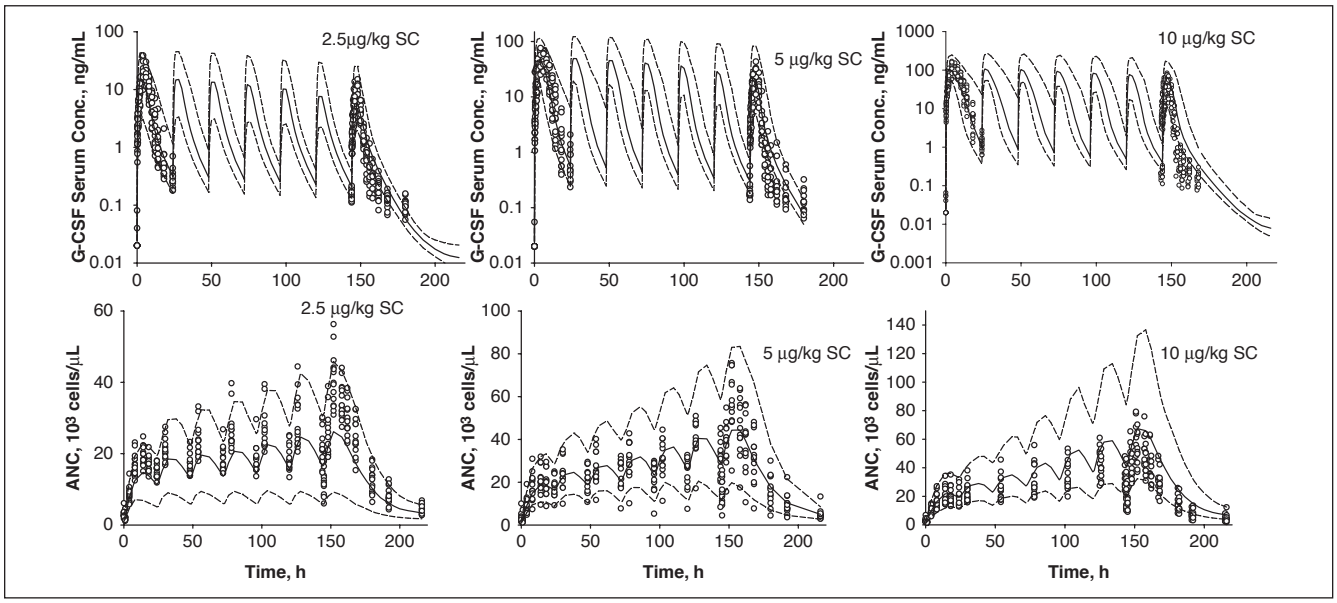

Figure 3. Time courses of filgrastim serum concentrations and ANCs (symbols) following multiple SC administrations of 2.5 µg/kg (left), 5 µg/kg (middle), and 10 µg/kg (right). The lines represent the 5th, 50th, and 95th percentiles of model-predicted values based on parameter estimates shown in Table III.

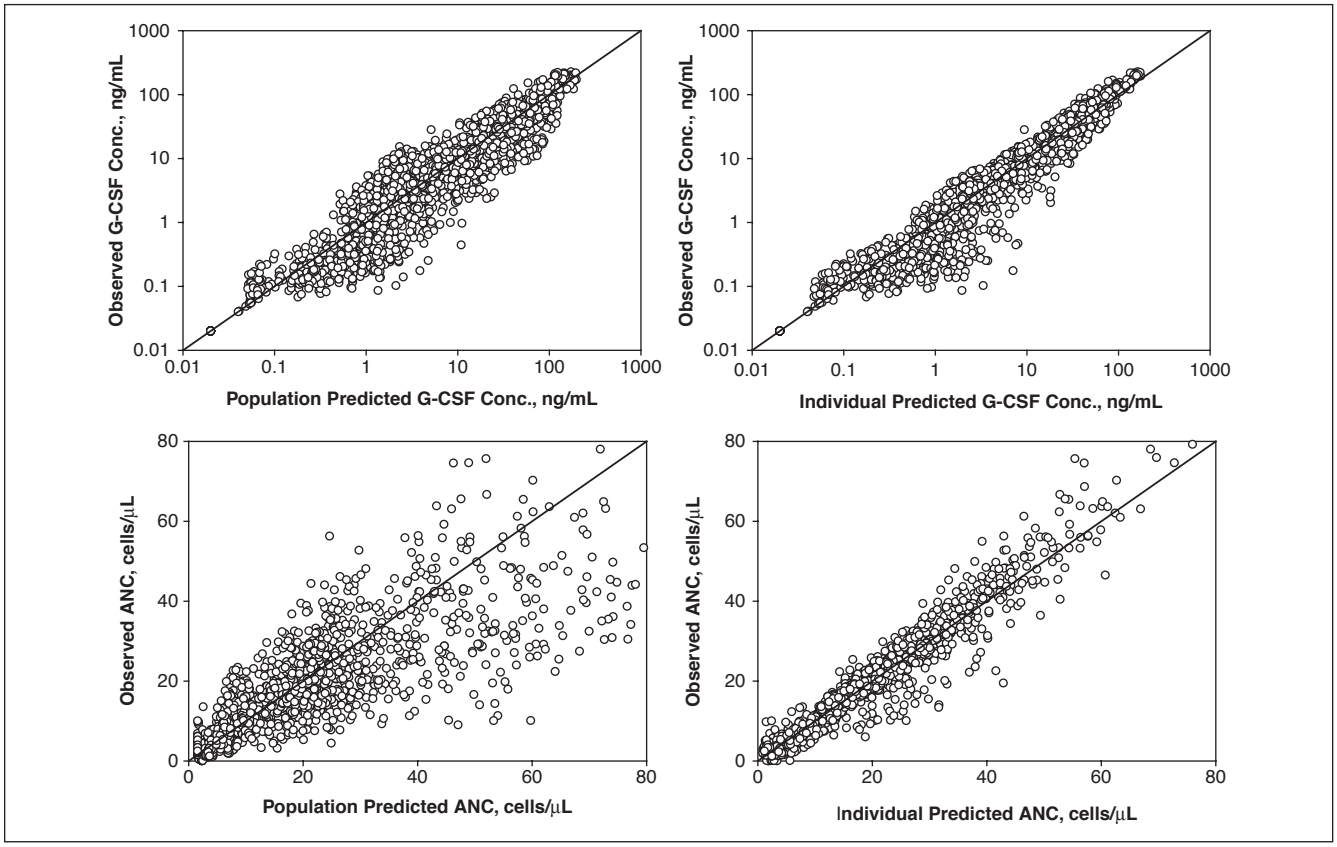

Figure 4. Diagnostic plots for assessment of goodness of fit.

These values are similar to ones reported by us previously despite introduced simplifications in the absorption model. Also, these estimates are consistent with analogous values for filgrastim published elsewhere.[12]

Only 3 parameters related to the receptor-mediated clearance of G-CSF were identifiable: the dissociation equilibrium constant K_D, internalization rate constant k_{int}, and number of G-CSFRs per cell ξ. The estimates of K_D and ξ reported in Table III are in the mass units consistent with the measured G-CSF concentration units. After conversion to molar units, K_D = 76.6 pM, and ξ = 5824 molecules/cell. The estimated K_D value is close to a value of 90.8 pM obtained by us from the in vitro Biacore-based binding assay (data not shown), and in the range of 70 to 150 pM reported elsewhere.[23,29] The estimated ξ value is larger than the number of G-CSF receptors per neutrophil, 50 to 500 reported in the literature.[1] This large value could account for non-specific binding or underestimation of neutrophils in the bone marrow. An estimate of the internalization rate constant k_{int} = 0.105 h^{-1} is much lower than the reported value of 6 h^{-1}.[30] This discrepancy might be because of neglecting a recycling of the drug-receptor complex in our model. Another confounding factor might be the dimerization of G-CSF receptors that occurs prior to internalization that was ignored by our TMDD model. The receptor binding parameters K_D and k_{int} were estimated with a relatively good precision, contrary to the estimate of ξ that had %RSE = 45.5%.

The pretreatment neutrophil count was estimated as $N_{B0} = 1.55 \cdot 10^3$ cells/μL, which is below the normal range of 1.8 to 7.7 10^3 cells/μL, and less than the mean value for studied subjects of $2.98 \cdot 10^3$ cells/μL. This is a consequence of the initial, short lasting decrease in ANC after dosing of filgrastim. The G-CSF dramatically up-regulates the affinity of neutrophil-endothelial cell homing receptor LAM-1,[31] which increases the fraction of the circulating neutrophils that marginate along the vessel walls causing a drop in the circulating cells. Our PD model does not account for the change in margination of neutrophils, and the low ANC values contribute to a smaller estimate of N_{B0}. The pool of neutrophils in the bone marrow at steady state, calculated from Equations 11 and 15, equals $N_{BM0} \cdot V_D = 228 \cdot 10^9$ cells. The production rate of

Table III Summary of Population PK-PD Parameters and Intersubject and Residual Error Variance Estimates of Filgrastim in Healthy Volunteers Following Intravenous and Subcutaneous Administrations

Parameter, Unit	Estimate	%RSE
Fixed effect		
θ_F	0.602	8.9
θ_{ka}, h^{-1}	0.651	6.3
θ_{kel}, h^{-1}	0.152	16.6
θ_{VD}, L	2.42	6.8
θ_{KD}, ng/mL	1.44	18.1
θ_{kint}, h^{-1}	0.105	7.8
$\theta\xi$, fg/cell	0.181	45.5
θ_{kmt}, h^{-1}	0.0728	9.7
θ_{kt}, h^{-1}	0.00862	60.2
θ_{NB0}, 10^3 cells/μL	1.55	17.9
θ_{SC50}, ng/mL	3.15	21.0
θ_{Smax1}	34.7	36.0
θ_{Smax2}	32.2	32.9
Interindividual variability		
ω^2_{kel}	0.194	33.1
ω^2_{VD}	0.138	25.9
$\omega^2\xi$	0.0587	65.6
ω^2_{SC50}	0.764	25.0
ω^2_{Smax1}	0.000188	133
ω^2_{NB0}	0.109	29.1
Residual variability		
σ^2_{addC}, $(ng/mL)^2$	0[a]	
σ^2_{propC}	0.259	6.3
σ^2_{addANC}, $(10^3$ cells/μL$)^2$	2.52	15.2
$\sigma^2_{propANC}$	0.0214	9.6

[a]Parameter was fixed.

precursor neutrophils is $k_{in} \cdot N_{BM10} \cdot V_D = 0.203 \cdot 10^9$ cells/h. The total neutrophil number in the blood and bone marrow at steady state is $(N_{B0} + N_{BM0}) \cdot V_D = 98.0 \cdot 10^9$ cells. This number can be used to assess the total number of G-CSFRs at the baseline as $R_{tot0} \cdot V_D =$ 333 pmol.

The number of transit compartments was determined based on the reduction of the minimum value of the objective function. For n = 4, the minimum value was 10121.4, and an additional transit compartment reduced it by 16.4. The number n = 9 resulted in a decrease of 3.0 from the minimum value for n = 8 compartments. Statistical significance of these changes was not tested. The transfer rate constant between transit compartments equals $k_t = 0.00862\ h^{-1}$. This corresponds to the transfer rate at steady-state conditions $k_t \cdot H_{20} = 0.0108\ h^{-1}$. The reciprocal of this value represents the mean transit time through each of the transit compartments, which can be used to calculate the mean residence time of neutrophil in the bone marrow as 836 hours (34.8 days). Such a large estimate of the neutrophil maturation time compared with the reported value of 8 to 13 days[6] is a consequence of a low k_t estimate. The low estimate of k_t is accompanied with the biggest relative standard error of all fixed effect parameters 60.2%. This seems to be a problem related to the model structure where the 3 parameters, S_{max2}, SC_{50}, and k_t, control a single transfer process that takes place in a hidden (not observable) compartment. Similar problems with estimating a transfer rate constant were reported for models describing stimulatory effects of erythropoietin.[32] In a published model of granulopoiesis, where G-CSF affects the transfer rates, one was not estimated but fixed at a physiological value.[15] The neutrophil elimination from the blood occurs at the rate $k_{mt} = 0.0728\ h^{-1}$ with the corresponding half-life $t_{0.5} = 9.52$ hours, which is close to the literature values of 6 to 7 hours.[5] The calculated mean blood residence time $1/k_{mt} = 12.8$ hours indicates that blood serves as a quick transit compartment for neutrophils before diapedesing. Estimates of the system parameters N_{B0} and k_{mt} had %RSE less than 20%. The maximal stimulation of neutrophils production $S_{max1} =$ 34.7. The maximum stimulation of the transit rate $S_{max2} = 32.2$. These rather high values are compensatory to the absence of the mobilizing effect of G-CSF in our model that contributes to the ANC on stimulation. The potency parameter SC_{50} was the same for both stimulatory processes and its estimate was 3.15 ng/mL (167 pM), which is close to the reported value of 4.72 ng/mL for a basic indirect model of the ANC response to filgrastim.[12] The %RSE for drug related parameters were in the range of 21.0% to 32.9%.

The selection of the IIV parameters were done according to the bottom-up approach starting from k_{el} and V_D, and expanding the set parameters until failure in the estimation process was observed. The estimation was valid only for successful minimization with a covariance step. The selected IIVs for k_{el}, V_D, ξ, SC_{50}, S_{max1}, and N_{B0} represent the largest set resulting in a stable parameter estimation. However, their estimated values are relatively high, resulting in wider confidence intervals for the model predicted values shown in Figures 2 and 3. The attempt to fix the extremely low estimate of IIV for S_{max1} at 0 resulted in a significant increase in the objective function value. The residual variability parameters were estimated with good precision. An estimate of the intercept in the

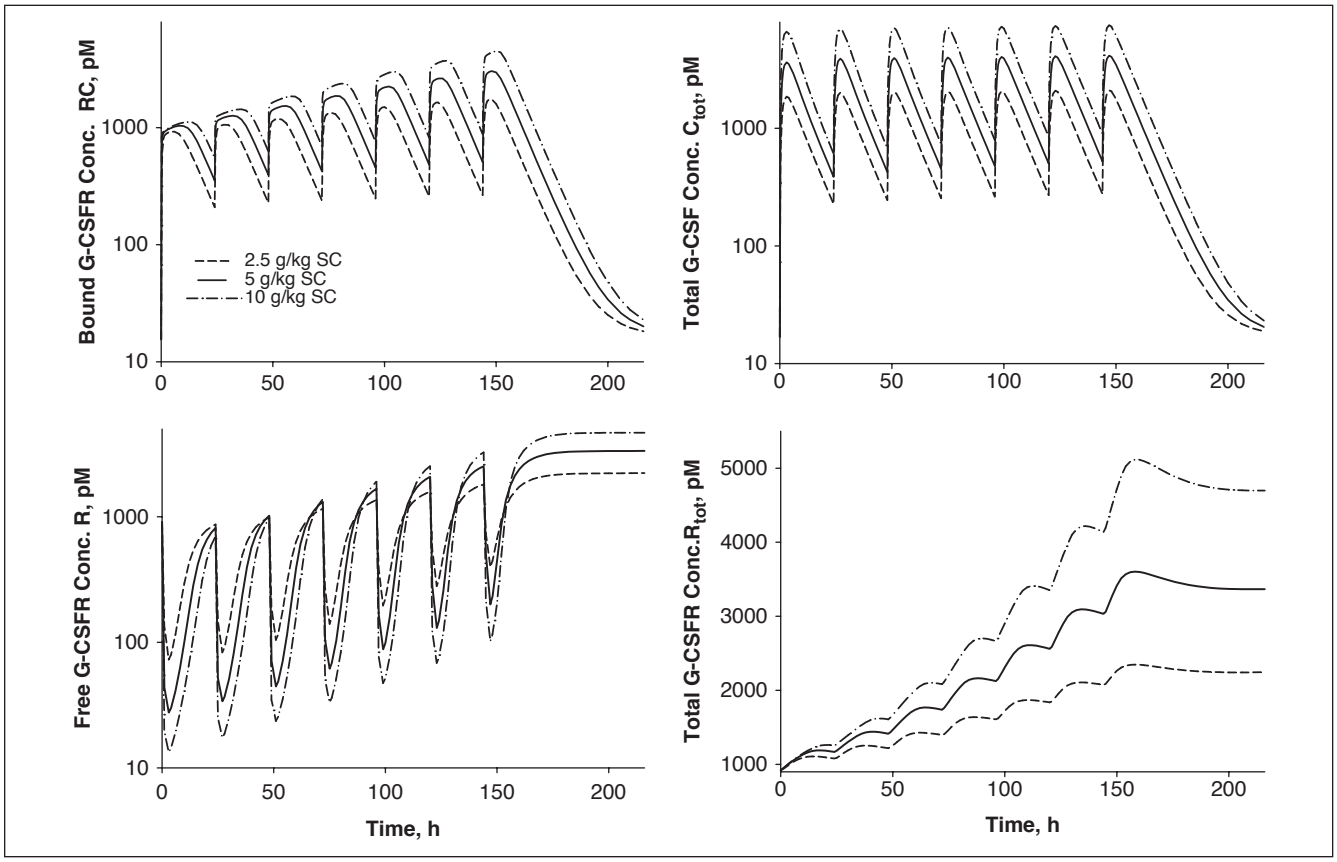

Figure 5. Simulated time profiles of bound G-CSF receptors RC, free G-CSF receptors R, total filgrastim concentrations C_{tot}, and total G-CSF receptor concentrations R_{tot}, following multiple SC administrations of 2.5, 5, and 10 μg/kg. The variables are expressed in pM units. Equations 5 and 6 were used to calculate RC and R_{rot}. R was calculated as R_{tot} - RC, and C_{tot} as C + RC. The parameter values used for simulations are shown in Table III.

additive model of RV for PK data was very small and was subsequently fixed at 0. The plots of individual estimates of the parameters above versus dose (supplementary material) showed that V_D and ξ estimates moderately increased with increasing dose. An apparent dose dependence of ξ indicates that the expression of G-CSF receptor on neutrophils increases with dose. An interpretation of the dose dependence of V_D is difficult because in the presented model there are several contributing factors such as increasing with dose and time the pool of G-CSF receptors, or the absence of the neutrophil marginalization. Since our model does not account for per cell receptor upregulation or margination, the estimates of V_D can compensate for a lack of these processes.

Figure 5 shows the simulated profiles of the PK model variables that were not measured, R, RC, C_{tot}, and R_{tot}. The time courses of the bound G-CSFR start at the baseline value of 15.5 pM and oscillate between troughs and peaks that increased following each SC dose to reach the level of 266 to 879 pM for the last trough and 1762 to 4395 pM for the last peak. After the seventh dose, the RC variable returned to the baseline within 72 hours. Similar patterns exhibit the total G-CSF serum concentration time profiles, except for a lack of increase in trough and peak values, which remain at the same level of 276 to 899 pM (troughs) and 2101 to 7528 pM (peaks) for each dose. The time courses for the free receptors are inverted and oscillate between the peaks and troughs with peaks and trough increasing for each dose to reach the levels of 1898 to 3255 pM for peaks and 102 to 397 pM for troughs. After the last trough, the R values increase to reach a plateau. This behavior is dictated by the G-CSFRs expressed on neutrophils in the bone marrow, which residence time was estimated to be much longer than a physiological one resulting in an artificial steady-state for R rather then a decline to the baseline value

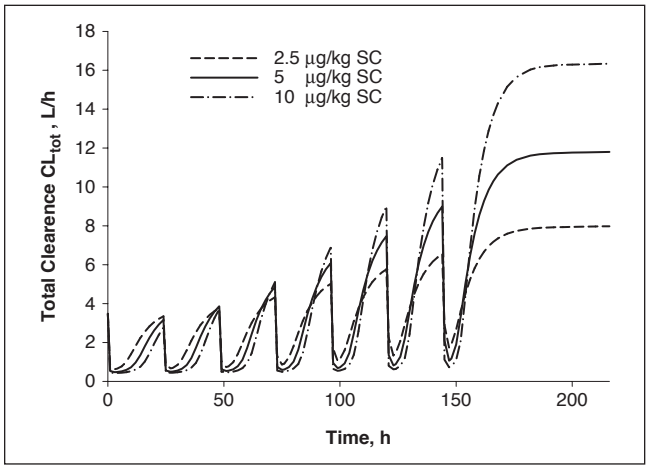

Figure 6. Simulated time profiles of the filgrastim total clearance CL_{tot} following multiple SC administrations of 2.5, 5, and 10 µg/kg. Equation 23 was used to calculate CL_{tot}. The parameter values used for simulations are shown in Table III.

of 907 pM. The amplitude of the decrease from the peak to the trough for R following each dose matches the amplitude of the increase from the trough to the peak for RC consistently with the receptor binding G-CSF molecules. The low levels of the troughs compared with the baseline indicate that after each dose almost all receptors are occupied. According to Equation 6, the time courses of the total receptors parallel the time courses of the total neutrophil count in the blood and the bone marrow. Consequently, one can observe an accumulation of R_{tot} that reaches the level of 2346 to 5114 pM to slowly decline to a baseline level. The rate of the decline is small for the same reasons provided for R.

The primary objective of this study was to establish a relationship between the receptor-mediated clearance of G-CSF and the neutrophil count in the bone marrow and blood. Equation 23 offers such a relationship with R_{tot} linked to the total neutrophils via Equation 6. The simulated time profiles for CL_{tot} on multiple SC dosing are shown in Figure 6. These curves seem to be scaled time profiles for free receptors R. This is indeed the case. One can use Equation 5 to show that:

$$R = R_{tot} - RC = \frac{R_{tot} \cdot K_D}{K_D + C} \qquad (24)$$

Then, Equation 23 can be transformed to the following form:

$$CL_{tot} = k_{el} V_d + k_{int} \cdot V_d \cdot \frac{R}{K_D} \qquad (25)$$

Equation 25 offers a straightforward interpretation of the impact of receptor binding on the total clearance. The decrease in free receptors after each dose administration causes a proportional decrease in total clearance of filgrastim. The clearance increases when the number of free receptors increases. The magnitude of the clearance increases with subsequent doses causing an observable decrease in filgrastim peak concentrations and AUC values.

DISCUSSION

The structure of the proposed PK-PD model is parsimonious given the data used for our analysis. The absorption model was reduced to a standard first-order process compared with our model for PK data only.[17] We also did not find it beneficiary to add a peripheral compartment that is present in PK-PD models of filgrastim published previously,[12] presumably because of the presence of the receptor-binding compartment. The physiologically present processes of mobilization of band and segmented neutrophils from the bone marrow, as well as the marginal pool, were tested and not included in the final model because of overparameterization. The neutrophil margination was modeled by others as a drug effect on the blood neutrophil dilution volume.[16] Because of the limited amount of information on the data, the initial decrease in ANCs following G-SCF administration was not modeled. This phenomenon was described in previous models as a temporal increase in filgrastim volume of distribution for neutrophils.[12]

Our major contribution to the existing PK-PD models for G-CSF was combining the receptor-mediated PK model with the PD model via our simplistic assumption that the total receptor pool size is proportional to the neutrophil count in the bone marrow and blood. Such an assumption to link the receptor compartment to the number of cells expressing it was proposed previously for a PK-PD model of pegylated thrombopoietin mimetic peptide effects on platelets.[33] Another mechanism was introduced that involved the modeling of the receptor turnover per cell and multiplying the receptor per cell by the number of neutrophils.[34] More empirical approaches have been applied previously where the receptor mediated clearance was modeled by means of the Michaelis-Menten equation with V_{max} proportional to the number of neutrophils.[12,15] In the view of the relationship between CL_{tot} and R_{tot} (Equation 23), this is fully justifiable based on the receptor-mediated disposition PK model. The relationships between Michaelis-Menten and TMDD parameters have been established as follows[35]:

$$V_{max} = k_{int} \cdot R_{tot} \cdot V_D \text{ and } K_m = K_D. \quad (26)$$

The present shortcomings of our model can be attributed to a too simplistic relationship between total receptors and total neutrophils. More mechanistic models of the link between receptors and the number of cells expressing them are necessary to account for different dynamics of these variables that are physically linked together. This is a subject for future studies.

The structural model describing the neutrophil dynamics is based on a previously introduced model where the maturation of the neutrophil precursors in the bone marrow is described by a sequence of transit (aging) compartments.[16] An alternative approach has been proposed to model the effect of lenograstim on neutrophil production in healthy volunteers.[36] There neutrophil maturation is described by a lifespan-based indirect model according to which cells exit the population at a rate determined by their lifespan. Lifespan-based PK-PD models have been successfully applied to describe the effects of other hematopoietic growth factors on red blood cells[37] and platelets.[33] The neutrophil data presented in this report can also be modeled using a lifespan-based PD model. The only limitation is lack of PK-PD software that can solve the lifespan-based model equations involving delays (delay differential equations). A numerical method adopted in PK-PD software that converts delay differential equations to ordinary differential equations[38] is poorly suited for the G-CSF-neutrophil system. Contrary to the red blood cell lifespan of 120 days and platelet lifespan of 10 days, the neutrophil lifespan in the circulation is about 7 hours. This implied a large number of differential equations for the transformed lifespan-model, PK-PD model, and consequently this approach has been abandoned.

In our PK-PD model, the stimulatory effect of filgrastim on neutrophil production and maturation is driven by the serum concentrations. A more mechanistic approach would involve the drug-receptor complex RC or receptor occupancy in accordance with the operational model of agonism.[39] We have not attempted to include one of these variables as a PD driving force. Such a modification would be desired, especially because it has been successfully implemented in the modeling of pharmacological effects of other hematopoietic agents.[22,33] This would enable a better understanding of the relationship between receptor affinity and filgrastim potency represented in our model by K_D and SC_{50}.

The PK-PD model presented here is meant to be used for modeling ANCs in response to an exposure to other agents that exhibit the same mechanism of action as G-CSF. These include biosimilar drugs to filgrastim, and other modified G-CSF molecules such as pegfilgrastim. Computer simulations can be used to apply the PK-PD for assessment of the impact of the receptor-mediated disposition in biosimilarity studies.[37] Another potential area for an application of the presented model is modeling the myelosupressive effects of anticancer agents with the administration of G-CSF as an adjuvant therapy. The bone structure of our PD model is very similar to models proposed by Frieberg et al.[28] An inclusion of a toxic effect on the proliferating bone marrow cells would be necessary. A hypothesis that the negative feedback present in these models is because of an accumulation of the G-CSF, as a consequence of the depletion of the receptor pool by chemotherapy, could be tested and, if accepted, this model component might be removed.

In summary, the presented model expanded previously published PK-PD models for filgrastim and pegfilgrastim by addition of the target mediated drug disposition. The increase in filgrastim clearance on multiple dosing was attributed to the increased neutrophil count in the bone marrow and blood paralleled by an increase in the total G-CSF receptor density. Simultaneous modeling of filgrastim plasma concentrations and ANC was necessary to adequately describe PK data. Simulations with varying PK and PD parameter values indicated that the presented model could be used for data of other granulopoiesis stimulating agents.

This study was supported by grants from Novartis Pharma AG and the Laboratory for Protein Therapeutics University at Buffalo.

Financial disclosure: The articles in this supplement are sponsored by the American Conference on Pharmacometrics.

REFERENCES

1. Demetri GD, Griffin JD. Granulocyte colony-stimulating factor and its receptor. *Blood*. 1991;78:2791-2808.

2. Anderlini P, Champlin RE. Biologic and molecular effects of granulocyte colony-stimulating factor in normal individuals: recent findings and current challenges. *Blood*. 2008;111:1767-1772.

3. Robinson CR. Reduce, reuse, and recycle. *Nat Biotechnol*. 2002; 20:879-880.

4. Skubitz KM. Neutrophilic leukocytes. In: Wintrobe MM, Greer J, eds. *Wintrobe's Clinical Hematology*. 11th ed. Philadelphia, PA: Lippincott, Williams, & Wilkins; 2004.

5. Bishop CR, Rothstein G, Ashenbrucker HE, Athens JW. Leukokinetic studies. XIV. Blood neutrophil kinetics in chronic, steady-state neutropenia. *J Clin Inv*. 1971;50:1678-1689.

6. McKenzie SB. *Textbook of Hematology*. Baltimore, MD: Williams and Williams; 1996.

7. Walte K, Gabrilove J, Bronchud MH, Platzer E, Morstyn G. Filgrastim (r-metHuG-CSF): the first 10 years. *Blood*. 1996;88: 1907-1929.

8. Spiekermann K, Roesler J, Emmendoerffer A, Elsner J, Welte K. Functional features of neutrophils induced by G-CSF and GM-CSF treatment: differential effects and clinical implications. *Leukemia*. 1997;11:466-478.

9. van Os R, van Schie ML, Willemze R, Fibbe WE. Proteolytic enzyme levels are increased during granulocyte colony-stimulating factor-induced hematopoietic stem cell mobilization in human donors but do not predict the number of mobilized stem cells. *J Hematother Stem Cell Res*. 2002;11:513-521.

10. Sung L, Dror Y. Clinical applications of granulocyte-colony stimulating factor. *Front Biosci*. 2007;12:1988-2002.

11. Borleffs JC, Bosschaert M, Vrehen HM, et al. Effect of escalating doses of recombinant human granulocyte colony-stimulating factor (filgrastim) on circulating neutrophils in healthy subjects. *Clin Ther*. 1998;20:722-736.

12. Wang B, Ludden TM, Cheung EN, Schwab GG, Roskos LK. Population pharmacokinetic-pharmacodynamic modeling of filgrastim (r-metHuG-CSF) in healthy volunteers. *J Pharmacokinet Pharmacodyn*. 2001;28:321-342.

13. Kuwabara T, Uchimura T, Kobayashi H, Kobayashi S, Sugiyama Y. Receptor-mediated clearance of G-CSF derivative nartograstim in bone marrow of rats. *Am J Physiol*. 1995;269:E1-E9.

14. Layton JE, Hockman H, Sheridan WP, Morstyn G. Evidence for a novel in vivo control mechanism of granulopoiesis: mature cell-related control of a regulatory growth factor. *Blood*. 1989;74: 1303-1307.

15. Foley C, Mackey MC. Mathematical model for G-CSF administration after chemotherapy. *J Theor Biol*. 2009;257:27-44.

16. Roskos LK, Lum P, Lockbaum P, Schwab G, Yang BB. Pharmacokinetic/pharmacodynamic modeling of pegfilgrastim in healthy subjects. *J Clin Pharmacol*. 2006;46:747-757.

17. Wiczling P, Lowe P, Pigeolet E, Ludicke F, Balser S, Krzyzanski W. Population phramacokinetic modelling of filgrastim in healthy adults following intravenous and subcutaneous administrations. *Clin Pharmacokinet*. 2009;48:817-826.

18. Levy G. Pharmacologic target-mediated drug disposition. *Clin Pharmacol Ther*. 1994;56:248-252.

19. Mager DE, Jusko WJ. General pharmacokinetic model for drugs exhibiting target-mediated drug disposition. *J Pharmacokin Pharmacodyn*. 2001;28:507-532.

20. Ng CM, Stefanich E, Anand BS, Fielder PJ, Vaickus L. Pharmacokinetics/pharmacodynamics of nondepleting anti-CD4 monoclonal antibody (TRX1) in healthy human volunteers. *Pharm Res*. 2006;23:95-103.

21. Mager DE, Jusko WJ. Receptor-mediated pharmacokinetic/pharmacodynamic model of interferon-beta 1a in humans. *Pharm Res*. 2002;19:1537-1543.

22. Woo S, Krzyzanski W, Jusko WJ. Target-mediated pharmacokinetic and pharmacodynamic model of recombinant human erythropoietin (rHuEPO). *J Pharmacokin Pharmacodyn*. 2007;34:849-868.

23. Jin F, Krzyzanski W. Pharmacokinetic model of target-mediated disposition of thrombopoietin. *AAPS Pharm Sci*. 2004;6:E9.

24. Sarkar CA, Lauffenburger DA. Cell-level pharmacokinetic model of granulocyte colony-stimulating factor: implications for ligand lifetime and potency in vivo. *Mol Pharmacol*. 2003;63:147-158.

25. Vainstein V, Ginosar Y, Shoham M, Ranmar DO, Ianovski A, Agur Z. The complex effect of granulocyte colony-stimulating factor on human granulopoiesis analyzed by a new physiologically-based mathematical model. *J Theor Biol*. 2005;234:311-327.

26. Roskos L, Cheung E, Vincent M, Foote M, Morstyn G. Pharmacology of filgrastim (r-metHuG-CSF). In: Morstyn G, Dexter TM, Foote M, eds. *Filgrastim (r-metHuG-CSF) in Clinical Practice*. New York: M. Dekker; 1998.

27. Mager DE, Krzyzanski W. Quasi-equilibrium pharmacokinetic model for drugs exhibiting target-mediated drug disposition. *Pharm Res*. 2005;22:1589-1596.

28. Friberg LE, Henningsson A, Maas H, Nguyen L, Karlsson MO. Model of chemotherapy-induced myelosuppression with parameter consistency across drugs. *J Clin Oncol*. 2002;20:4713-4721.

29. Avalos BR, Gasson JC, Hedvat C, et al., Human granulocyte colony-stimulating factor: biologic activities and receptor characterization on hematopoietic cells and small cell lung cancer cell lines. *Blood*. 1990;75:851-857.

30. Sarkar CA, Lowenhaupt K, Horan T, Boone TC, Tidor B, Lauffenburger DA. Rational cytokine design for increased lifetime and enhanced potency using pH-activated "histidine switching." *Nature Biotech*. 2002;20:908-913.

31. Spertini O, Kansas GS, Munro JM, Griffin JD, Tedder TF. Regulation of leukocyte migration by activation of the leukocyte adhesion molecule-1 (LAM-1) selectin. *Nature*. 1991;349:691-694.

32. Krzyzanski W, Jusko WJ, Wacholtz MC, Minton N, Cheung WK, Pharmacokinetic and pharmacodynamic modeling of recombinant human erythropoietin after multiple subcutaneous doses in healthy subjects. *Eur J Pharm Sci*. 2005;26:295-306.

33. Samtani MN, Perez-Ruixo JJ, Brown K, Cerneus D, Molloy C. Pharmacokinetic and pharmacodynamic modeling of pegylated thrombopoietin mimetic peptide (PEG-TPOm) after single intravenous dose in healthy subjects. *J Clin Pharmacol*. 2009;49: 336-350.

34. Jonsson EN, Macintyre F, James I, Krams M, Marshall S. Bridging the pharmacokinetics and pharmacodynamics of UK-279,276 across healthy volunteers and stroke patients using mechanistically based model for target-mediated disposition. *Pharm Res*. 2005;22:1236-1246.

35. Yan X, Mager DE, Krzyzanski W. Selection between Michaelis-Menten and target-mediated drug disposition pharmacokinetic models. *J Pharmacokinet Pharmacodyn*. 2010;37: 25-48.

36. Krzyzanski W, Ramakrishnan R, Jusko WJ. Basic models for agents that alter production of natural cells. *J Pharmacokin Biopharm*. 1999;27:467-489.

37. Ramakrishnan R, Cheung WK, Wacholtz MC, Minton L, Jusko WJ. Pharmacokinetic and pharmacodynamic modeling of recombinant human erythropoietin after single and multiple doses in healthy volunteers. *J Clin Pharmacol*. 2004;44:991-1002.

38. Perez-Ruixo JJ, Kimko HC, Chow AC, Piotrovsky W, Krzyzanski W, Jusko WJ. Population cell lifespan models for effects of drugs following indirect mechanism of action. *J Pharmacokin Pharmacodyn*. 2005;32:767-793.

39. Black JW, Leff P. Operational models of pharmacological agonism. *Proc R Soc Lond B Biol Sci*. 1983;220:141-162.